

Transparent flexible conductor of poly(methyl methacrylate) containing highly-dispersed multiwalled carbon nanotube

Dong Ouk Kim ^a, Min Hye Lee ^a, Jun Ho Lee ^a, Tae-Woo Lee ^b,
Kwang Jin Kim ^c, Young Kwan Lee ^d, Taesung Kim ^e,
Hyoun Ryeol Choi ^e, Ja Choon Koo ^e, Jae-Do Nam ^{a,*}

^a Department of Polymer Science and Engineering, SAINT, Sungkyunkwan University, Suwon 440-746, Republic of Korea

^b Samsung Advanced Institute of Technology (SAIT), Suwon, Republic of Korea

^c Department of Mechanical Engineering, University of Nevada, Reno, NV 89557, USA

^d Department of Chemical Engineering, Sungkyunkwan University, Suwon 440-746, Republic of Korea

^e School of Mechanical Engineering, Sungkyunkwan University, Suwon 440-746, Republic of Korea

Received 5 June 2007; received in revised form 6 July 2007; accepted 10 July 2007

Available online 1 August 2007

Abstract

Multiwalled carbon nanotubes (MWCNTs) were incorporated into a poly(methyl methacrylate) (PMMA) solution to develop a transparent and flexible composite conductive film. Monitoring the MWCNT-granule size in the PMMA solutions as well as after the film casting, the self-aggregation of MWCNTs was thoroughly investigated to provide a highly-dispersed polymeric conductor. In addition to the degree of acid treatment of MWCNTs, the dipole moment of solvent and the random-coil length of polymer were considered to be the key factors for the MWCNTs to retain the highly-dispersed state in the polymer matrix after solidification. Investigating several solvent systems, dimethylformamide was found to have the best dispersing capability for the MWCNT/PMMA system to give a surface electrical conductivity up to 10^{-2} S/cm at ca. 3.0 wt% of MWCNT, which was considered to be well above what had been reported for such a low level of MWCNT loading, with a light transmittance over 95%. Finally, the polymer-rich layer, which is usually formed on the coating surface due to the surface tension and wetting characteristics of the MWCNT/PMMA mixture, was mechanically peeled off to give an increase in electrical conductivity of nearly two orders of magnitude.

© 2007 Elsevier B.V. All rights reserved.

PACS: 72.60.+g; 72.80.-r; 73.25.+i; 74.25.Gz; 78.66.-w

Keywords: Multiwalled carbon nanotubes (MWCNTs); Conductive polymer film; Dispersion; Conductivity; Percolation

1. Introduction

Since carbon nanotubes were first reported in 1991 by Iijima [1], they have been intensively

* Corresponding author. Tel.: +82 31 290 7285; fax: +82 31 292 8790.

E-mail address: jdnam@skku.edu (J.-D. Nam).

investigated due to their mechanical, chemical and electrical properties [2–4]. Carbon nanotubes (CNTs) are considered as functional additives in polymeric composites systems. In particular, when compared with other spherical-shaped conductive filling materials such as carbon black and silver particle, their relatively large length/diameter aspect ratios help the composite systems show a high electric conductivity at low concentrations of the carbon nanotubes, due to their low percolation threshold [5,6]. Although CNTs have excellent properties in nature, their dispersion characteristics specifically incorporated in various binding systems still remain as a challenge to be required for the optoelectronic device fabrication and assembly processes.

Curran et al. reported the electrical conductivity as about 10^{-4} S/cm at 35 wt% loading of single-walled carbon nanotubes (SWCNT) in poly(*m*-phenylenevinylene-co-2,5-dioctoxy-*p*-phenylenevinylene) [6]. It was reported that the poly(phenyleneethynylene) (PPE)-functionalized SWCNT was soluble in organic solvents and the electrical conductivity of PPE-SWCNT/polycarbonate composite system reached 4.81 S/cm at 7 wt% of SWCNT loading [7]. Recently, there was a report on the SWCNT/PMMA composite system giving the electrical conductivity of 10^{-6} S/cm at 2 wt% of SWCNT loading [8]. For MWCNT/polyimide composite systems, Ogasawara et al. reported 10^{-4} – 10^{-2} S/cm of electrical conductivity with 3.3–14.3 wt% of MWCNT loading [9], and Zhu et al. reported 10^{-10} – 10^{-5} S/cm at around 1–12 wt% of MWCNT loading [10]. The electrical conductivity of a water-soluble composite system, MWCNT/PVA (poly vinyl alcohol), was reported as 10^{-2} S/cm with 3 wt% of MWCNT loading [11]. For transparent applications, the electrical conductivity of the H_2O_2 -treated MWCNT/polycarbonate(PC) composite system was 10^{-1} S/cm at 7 wt% loading of peroxide-treated MWCNT [12]. The electric sheet resistivity of the MWCNT/PMMA composite system reached 10^3 Ω /square at 1 wt% of MWCNT loading using UV-ozone treatment for MWCNT [13].

Reviewing previously-reported results, CNT/polymer composite systems show a wide range of electrical conductivities in a wide range of CNT loading, which makes it difficult to identify the key factors of the electrical threshold. It is often found that different researchers provide different values of electrical conductivity and light transmittance for the same material systems. Furthermore,

it should be pointed out that those reported values are not always reproduced by different researchers. Those discrepancies in electrical conductivities may be due to the non-uniform spatial distribution of carbon nanotubes in the states of liquid mixtures or solidified forms. As well known, CNTs are hardly dispersed and easily agglomerate to form various-sized granules, which could influence the electrical conductivity and transparency to a great extent. The agglomerated CNTs usually require additional amount of CNT loading to reach the electrical percolation state and the CNT-agglomerated spots could become a serious defect in various optoelectronic applications.

The percolation threshold for the electrical conductivity has been investigated to depend on the aspect ratio [14], alignment [15], and dispersion [16]. In particular, MWCNTs have an extremely large surface area with the van der Waals attraction and, thus, they easily self-aggregate in polymeric solutions [17–19]. There have been many attempts to obtain a homogeneous, fine, and stable dispersion of carbon nanotubes in polymeric composites [20,21]. Several mechanical and chemical techniques have been introduced, despite the lack of understanding of the dispersion and stability of nanotubes in polymeric solutions [8]. The mechanical dispersion methods include a high shear mixing known as melt blending, which is relatively easier than the other methods, yet not efficient, because of the high viscosity of the composites even at low concentrations of the nanotubes [22]. In the case of chemical techniques, the open-end functionalization method is most widely used, which involves refluxing the CNTs in nitric acid, whereupon the carboxylic groups which are formed on the CNT surfaces are converted into other functional groups via standard condensation reactions [23,24]. Functionalization techniques of the CNT sidewalls have been reported to use such organic reagents as azomethine ylides, carbenes, nitrenes, aryl radicals and diazonium to disperse CNTs in various polymer systems [25–30]. However, the CNT dispersion is yet to be understood in relation with the functionalization of CNT sidewalls.

Although CNTs look dispersed well in the solution state right after the physical mixing, they often give CNT sediments or floating granules after being placed still for a time being. Unless there is a good compatibility among the solvent, polymer and CNTs, we believe that the CNT

granule size grows in the polymeric solution with time to reach a critical granule size for sedimentation. In addition, although a well-dispersed CNT mixture is used, the CNTs could easily agglomerate to form CNT grains while being solidified by the solvent evaporation in the drying process of film casting.

In this study, we carefully investigated the MWCNT dispersion in various PMMA polymer solutions by measuring the dispersed granule size of MWCNT using a dynamic light scattering technique, which was correlated well with visual observation and light transmittance of the solution mixtures. The acid treatment conditions and different solvent type were studied in relation with the electrical conductivity, aggregated-MWCNT granule, and light transmittance of coated thin films. The surface morphology of MWCNT/PMMA coating was mechanically modified by peeling off the polymer-rich layer subsequently to give an enhanced electrical pathway of MWCNTs.

2. Experimental

2.1. Multiwalled carbon nanotubes

The multiwalled CNTs synthesized by the thermal chemical vapor deposition (CVD) method were purchased from Iljin Nanotech Co., Korea. The diameters, lengths of the carbon nanotubes and number of multiwalled shells were measured by TEM (JEM-3011 TEM, JEOL Tokyo, Japan) to give about 10–20 nm in outer diameter, 1–10 μm in length, and ca. 17 walls (Fig. 1). The impurity content estimated by thermo-gravimetric analysis was approximately 5 wt% (TGA, DuPont, Ltd., TGA 2910, USA).

The MWCNTs were heat treated in an oxygen-flowing environment to remove amorphous carbon impurities. The optimum heat treatment temperature was determined by using TGA to prevent the thermal degradation of the carbon nanotubes. The pre-treatment time, treatment temperature, ramping and oxygen flow rate were 1 h, 663 K, 5 K/min and 40 standard cubic centimeters per minute (SCCM), respectively.

After the heat treatment, an acid treatment was used to remove metallic catalyst impurities. The MWCNTs were sonicated for several hours in a (3:1) mixture of concentrated sulfuric (98%) and hydrochloric (100%) acid at a frequency of 20 kHz. The sonication time was 12, 18, and 24 h. Finally, the MWCNTs were subjected to centrifugation at a speed of 12,000 rpm for 20 min and then rinsed with water repeatedly using a PTFE filter with a pore size of 0.2 μm . The Raman spectra were obtained using an FT-Raman spectrometer (Model: FRA 106/S, Bruker Optics, Germany) to check the effects of the acid treatment time on the efficiency of functionalization.

2.2. Polymer matrix systems

5 wt% of polymethylmethacrylate (PMMA) ($M_w = 350,000$ g/mol, 1.15 g/cm³, Sigma–Aldrich) was dissolved in four different solvent systems: chloroform, toluene, tetrahydrofuran (THF), and dimethylformamide (DMF) with a mechanical stirrer. The purified MWCNTs were dispersed in a 5 wt% solution of PMMA for four different solvent systems and sonicated for several hours at a frequency of 20 kHz. For comparison, in this study, a semi-crystalline transparent polymer, PVDC copolymer (poly(vinylidene chloride-co-acrylonitrile-co-methyl

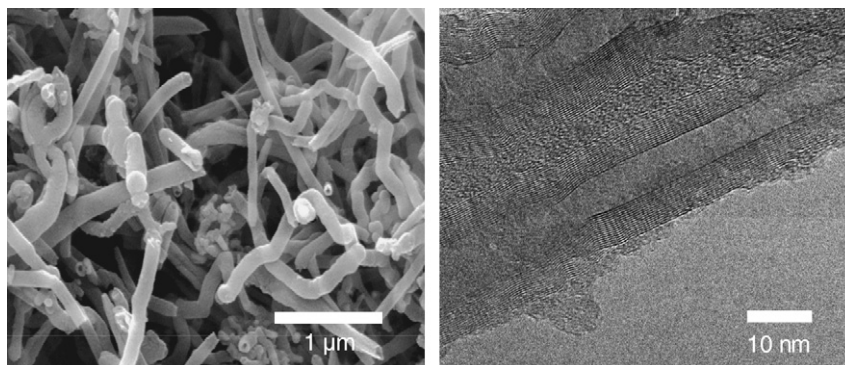


Fig. 1. SEM and TEM micrographs of MWCNTs.

methacrylate)) ($M_w = 90,000$ g/mol, 1.68 g/cm³, Sigma–Aldrich), was investigated using DMF as a solvent (PVDC/DMF weight ratio: 0.05, MWCNTs/PVDC weight ratio: 0.005).

2.3. MWCNT dispersion

The solution dispersion of the MWCNTs was visually examined using optical microscopy (Olympus Inc., Japan) and UV–Vis–NIR spectroscopy (Model: Cary 50, Varian Inc., USA). Dynamic light scattering (DLS, Model: DLS-7000, Otsuka Electronics, Japan) experiments were performed for the MWCNT/PMMA/DMF mixture having a MWCNT/PMMA weight ratio as 0.025 and a PMMA/DMF weight ratio as 0.0006. The dilute mixture was aged at ambient temperature for two weeks to evaluate the stability of the dispersion before the DLS experiments.

2.4. Electrical conductivity

The MWCNT/PMMA/DMF mixtures were prepared for the measurement of electrical conductivity maintaining the PMMA/DMF weight ratio at 0.05 varying the MWCNT contents with respect to PMMA from 0 wt% to 3.0 wt% in increments of 0.5 wt%. Thin composite films were cast on the surface of the poly(ethylene terephthalate) (PET) film as well as glass plate using a solvent casting method. Prior to the solvent casting, the PET film was treated with an oxygen plasma (250 W and 150 mTorr, 30 s.) and the glass plate was cleaned and coated with hexamethyldisilazane (Model: AZ AD Promoter-K, AZ Electronics Materials, Luxembourg) to enhance the adhesion between the composite films and the substrates. The electrical conductivity was monitored by a 4-point type probe (Model: Universal probe, Jandel Inc., USA) connected to a current/voltage source-measure unit (Model: Keithley 236, Keithley Instruments Inc., USA). The contact pressures between the probe needle and the film surface were carefully controlled by means of a tension knob to prevent the surface from being damaged by the needle. The contact pressure was approximate 15 g/cm².

The MWCNT/PMMA composite films were mechanically polished using micro-fiber pad and alumina powder (diameter: 0.3 μ m, Model: XL16756, Excel technologies Inc., USA) to enhance the electrical contact between the MWCNTs and

the probes of the 4-point probe instrument. The surface morphology of the polished surface was investigated by scanning electron microscopy (Model S-2400, Hitachi Inc., Japan).

3. Results and discussion

3.1. Effects of acid-treatment time

The Raman spectra of the carbon nanotubes are shown in Fig. 2. The prominent D (at around 1290 cm⁻¹) and G (at around 1590 cm⁻¹) band peaks clearly indicate the intrinsic characteristics of the carbon nanotubes. The carbon nanotubes exhibit a strong tangential mode band at ca. 1590 cm⁻¹ and a weak band at ca. 1290 cm⁻¹, which is attributed to the sp-3 hybridized carbon in the hexagonal framework of the nanotube walls [31]. As the acid treatment time increases from 12 to 24 h, the peak intensity increases in the region around 3300 cm⁻¹ (more exactly: 3370–3470 cm⁻¹), which corresponds to the O–H stretching in carboxylic groups on the MWCNT surface. There is an apparent increase in the peak intensity at 3300 cm⁻¹ with the acid treatment time of MWCNTs. As the acid treatment time increases, the CNT length is decreased and, subsequently, the probability of functionalization tends to increase [23]. Accordingly, our results demonstrate that the MWCNTs are shortened and their sidewalls are substantially functionalized by the acid treatment after 24 h.

3.2. Dispersion of MWCNT/polymer solution mixtures

In this study, MWCNT dispersion was investigated for four different types of solvent (chloroform, toluene, THF and DMF) and two polymer systems (PMMA and PVDC). When a black and uniform ink-type appearance is observed, the MWCNTs can be regarded as being dispersed well in the polymer solutions. On the other hand, if the MWCNT dispersion is not good, some of the MWCNTs are sedimented at the bottom of the solution mixture and the color becomes lighter black.

The MWCNT/polymer solution mixtures are compared in Fig. 3a and b before and after sonication, respectively. Fig. 3c shows the aged mixtures after 24 h of sonication treatment. As shown in Fig. 3a, all the acid-treated MWCNTs are not dis-

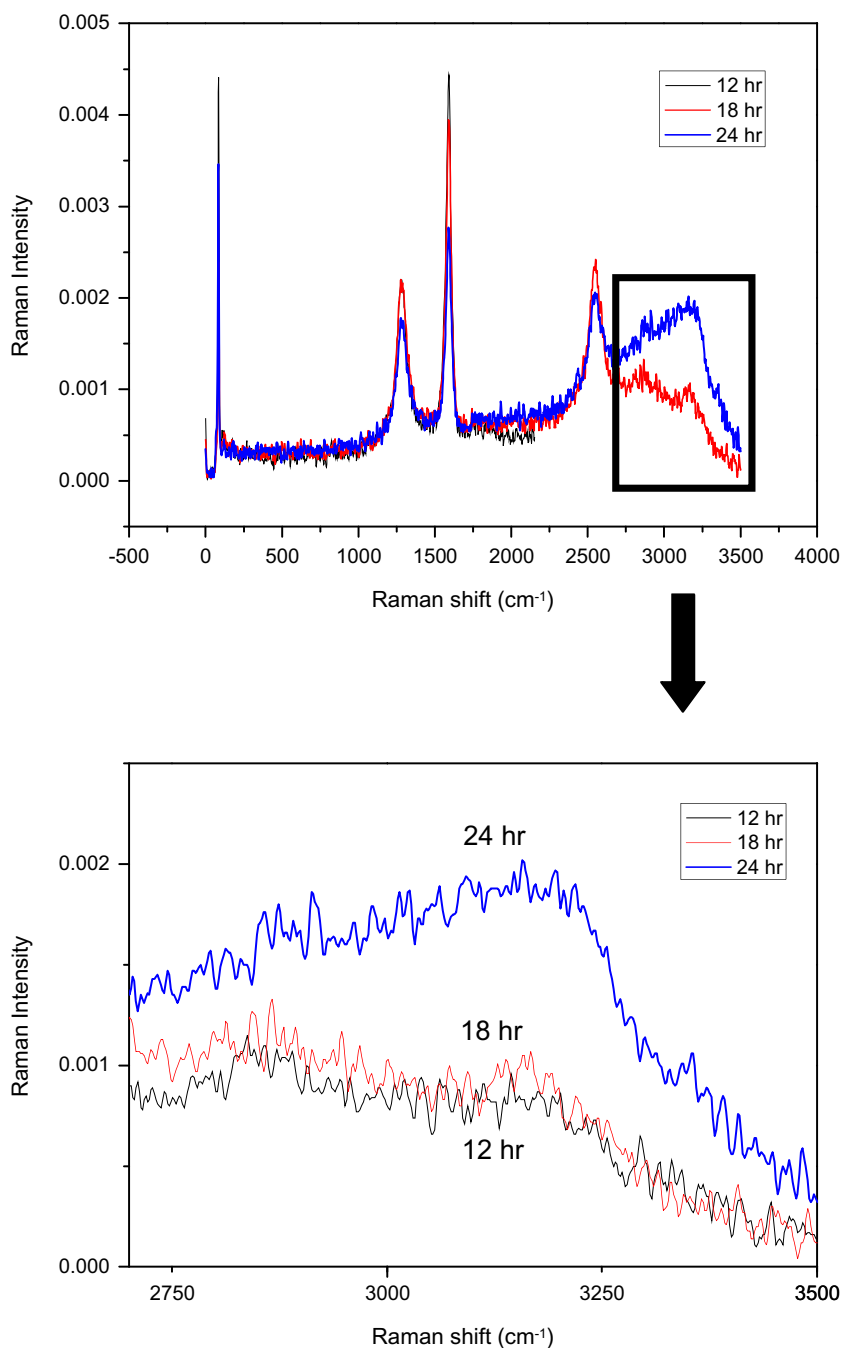


Fig. 2. Raman spectra of MWCNTs for various acid treatment conditions.

persed in the organic solvents before the sonication treatment to form granules at the bottom of the bottles as the arrow indicated in figures. After sonication in Fig. 3b, the MWCNTs look as being dispersed well in all the polymer solutions, although there are a slight difference in color and uniformity among samples. At a glance, the sonication process

seems to be an efficient way in dispersing MWCNTs in organic solvents. However, after 24 h of aging following the sonication process, the MWCNTs begin to agglomerate and sediment as can be observed in Fig. 3c for the samples in chloroform, toluene, and THF. These three solvent systems exhibit different colors and different amounts of

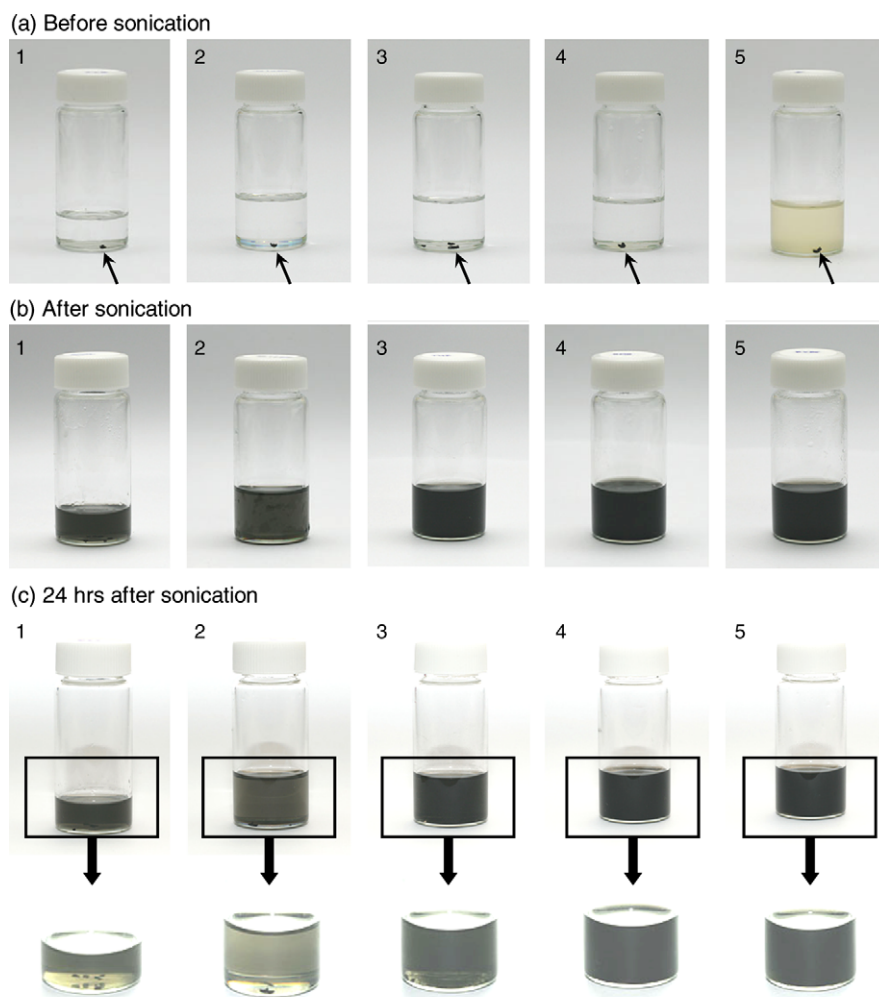


Fig. 3. Visual observation of MWCNT polymer mixtures (a) before sonication, (b) after sonication, and (c) aged for 24 h after sonication. The samples indicated are 1: MWCNT/PMMA/chloroform, 2: MWCNT/PMMA/toluene, 3: MWCNT/PMMA/THF, 4: MWCNT/PMMA/DMF and 5: MWCNT/PVDC/DMF.

sedimentation, indicating different dispersing capability. Apparently, the DMF system shows no sedimented MWCNT granules and maintains as a homogeneous mixture after 24 h of aging. The order of dispersion capability in the visual examination, which is based on the color and amount of sedimentation, is DMF > THF > chloroform > toluene. The physical dispersion of sonication, which is most commonly used in CNT dispersion, usually provides a good-looking mixture for a short period of time, but the long-term stability should be checked for following downstream fabrication processing.

Further evaluation of the MWCNT dispersion was performed using UV–Vis–NIR transmittance and optical microscopy. The UV–Vis–NIR transmittances of samples in Fig. 3c, which are aged

for 24 h after sonication, are compared in Fig. 4. A well-dispersed mixture provides darker color in visual observation, which should correspond to a lower value in transmittance intensity. Low transmittance is due to the diffusion of light by the well-dispersed particles in the solution mixture, indicating that MWCNTs are well-dispersed. The DMF system, which was darkest in color in Fig. 3c, exhibits 89% of transmittance at 380 cm^{-1} of wavenumber (Fig. 4), whereas the chloroform and toluene systems show pale gray and about 95% of transmittance. According to Fig. 4, the order of transmittance intensity is toluene > chloroform > THF > DMF, which apparently agrees with the order of the dispersion capability examined in visual observation.

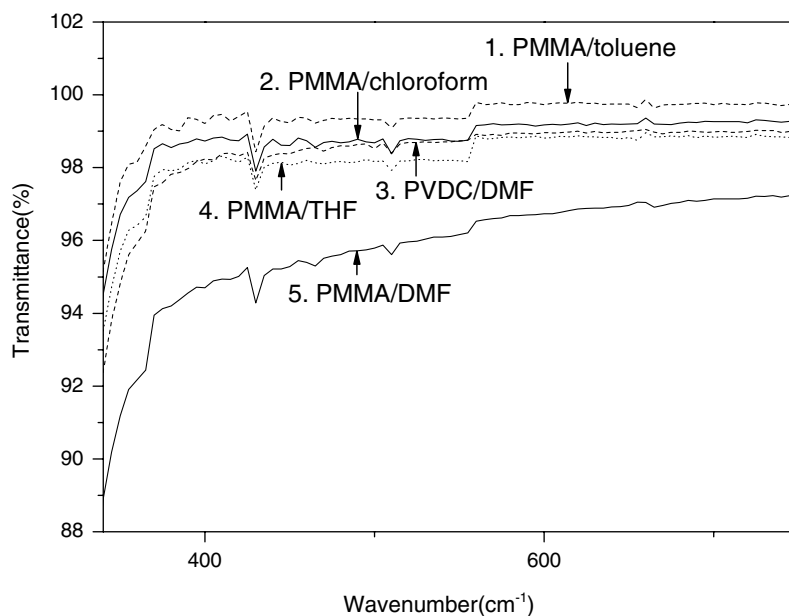


Fig. 4. Visible-ray transmittance of MWCNT polymer mixtures indicating 1: MWCNT/PMMA/toluene, 2: MWCNT/PMMA/chloroform, 3: MWCNT/PVDC/DMF, 4: MWCNT/PMMA/THF, 5: MWCNT/PMMA/DMF.

The optical microscopy images for the MWCNT/polymer film are shown in Fig. 5 for the samples corresponding to those examined in Fig. 3b. The chloroform (Fig. 5a) and toluene (Fig. 5b) mixtures show noticeable MWCNTs agglomerates in PMMA mixture. The MWCNT agglomerate size in chloroform and toluene are relatively smaller than that in THF (Fig. 5c). There are no agglomerates observed in the MWCNT/PMMA/DMF mixture, indicating

that DMF have the best dispersion ability among the solvents, which agrees well with results in visual observation and light transmittance. Although DMF is the best solvent for PMMA, it is not the case for the PVDC polymer system as seen in Fig. 5e. In the MWCNT/PVDC/DMF system, MWCNTs look well-dispersed in visual examination (Fig. 3) and transmittance (Fig. 4), but a loosely-agglomerated granules can be observed in Fig. 5e. Accordingly, it

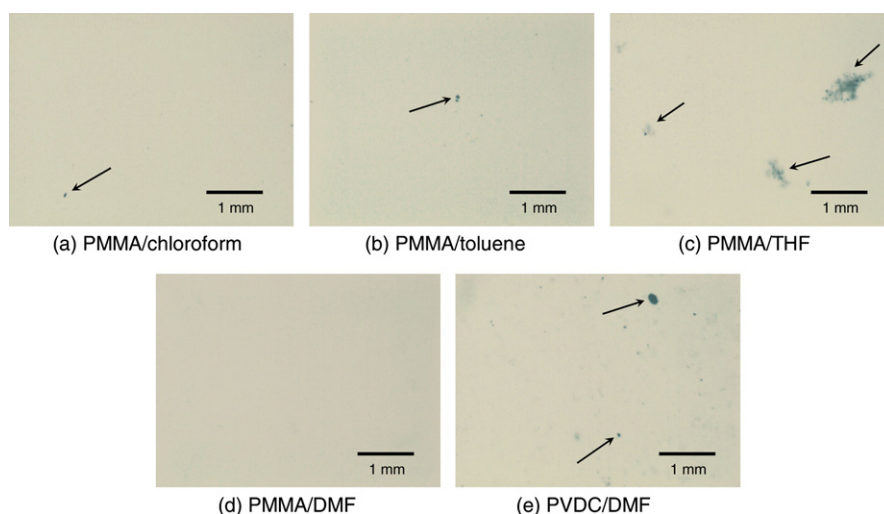


Fig. 5. Optical micrographs of MWCNT polymer mixtures coated on glass substrate comparing (a) MWCNT/PMMA/chloroform; (b) MWCNT/PMMA/toluene; (c) MWCNT/PMMA/THF; (d) MWCNT/PMMA/DMF and (e) MWCNT/PVDC/DMF. All samples were prepared at the same mixing ratios of MWCNTs/PMMA as 0.005, and polymer/solvent as 0.05.

should be mentioned that different polymer gives different dispersion for the same solvent to be used in CNT mixtures.

DMF turns out to be the most effective solvent system to disperse the MWCNTs in the PMMA solution among four different types of solvents investigated in this study. DMF and THF are classified as polar aprotic solvents, whereas toluene and chloroform are classified as non-polar (lipophilic) solvents, which may be represented by the dipole moment. The dipole moment values of these four solvents are 3.820 D for DMF, 1.750 D for THF, 1.040 D for chloroform and 0.375 D for toluene [32]. Although detailed mechanism is not clear yet, it may be reasonably speculated that the dipole-dipole interaction among the solvent molecule, carboxylic groups in MWCNT, and polar groups in PMMA chains. The order of the dipole moment values consists with the dispersion capability estimated by visual observation and transmittance measurement. Subsequently, we consider that the solvent polarity is closely associated with the MWCNT dispersion in PMMA solution.

From the viewpoint of physical interaction of polymer chains and MWCNTs, the MWCNT dispersion in polymers may be evaluated by comparing the dimensions of the polymer chain and MWCNT in the molecular level [8]. The average radius of gyration of the isolated PMMA chains in a dilute solution may be expressed as $\langle S^2 \rangle = a(M_w)^b$, where $\langle S^2 \rangle$ is the mean-squared radius of gyration in the unit of 0.01 nm^2 . M_w is the molecular weight of PMMA, and the constants a and b for PMMA are 0.0713 and 1.0098, respectively [8]. Using the above equation, the average diameter of a random coil may be estimated by $2\langle S^2 \rangle^{1/2}$. For the PMMA system with $M_w = 350,000 \text{ g/mol}$ in this work, the average diameter of PMMA coil may be estimated to be 34 nm. However, the molecular weight of PVDC used in this study is 90,000 g/mol, which gives the estimated average diameter of PVDC random coil is 7.3 nm. Consequently, the average diameter of PMMA coil is about 3.4 times larger than that of the carbon nanotubes (ca. 10 nm), whereas that of the PVDC random coil is even shorter than the diameter of the carbon nanotubes. Therefore, it may be reasonable to mention that the PMMA coil is long enough to be capable of wrapping up the carbon nanotubes effectively to prevent the agglomerations of nanotubes bundles, which is not the case with PVDC. This consideration agrees with the observed dispersion of PMMA and PVDC

systems in color (Fig. 3), transmittance (Fig. 4) and agglomerates (Fig. 5).

As a result, dispersion of MWCNTs in polymer seems substantially influenced by polymer type, molecular weights (or chain lengths) of polymer, and the polarity of solvent. However, the precise dispersion control and interaction mechanism is far from being clearly understood and further study is required for various polymer/solvent systems.

3.3. Dynamic light scattering (DLS) analysis

The degree of CNT dispersion has been measured by the dynamic light scattering (DLS) method in ethanol [33] and DI water [34,35] to estimate the length distribution of dispersed carbon nanotubes [36,37]. DLS detects the intensity fluctuation of the scattered light due to the Brownian motion of the dispersed particles. The estimation of the size of objects is made from the measured intensity, $I(\tau, t)$, to give the auto-correlation function, $G_2(\tau)$, viz: $G_2(\tau) = [I(t) \times I(t + \tau)] / [I(t)]^2$, where t is the detecting time and the τ is correlation time. The normalized first-order auto-correlation function, $g_1(\tau)$ is given by $g_1(\tau) = \sqrt{G_2(\tau) - 1}$. Subsequently, the function $g_1(\tau)$ is related to the diffusion coefficient of the particles, viz: $g_1(\tau) = B \exp(-D(\tau)q^2)$, where q is the scattering vector ($q = 4\pi n \times \sin(\theta/2)/\lambda$) and D is diffusion constant. Here, n is the refractive index, θ is the scattering angle, and λ is the wavelength in a vacuum. Finally, the size of the dispersed particles is calculated from the diffusion coefficient through the Stokes–Einstein equation, $R = k_B T / 6\pi\eta D$, where R is the particle radius, k_B is the Boltzmann constant, T is the absolute temperature, and η is the solvent viscosity. In this way, the final size distributions of our MWCNT/PMMA/DMF mixtures were obtained from the function $G_2(\tau)$ by the inverse Laplace transformation [35]. Accordingly, the number of particles and the laser intensities are shown in Fig. 6 for the MWCNT mixtures after 12, 18 and 24 h of acid-treatment.

In DLS measurement, the agglomerated MWCNT bundles may well give a relatively larger size than the well-dispersed nanotubes. Accordingly, it is reasonable to suppose that the size distributions in Fig. 6, which are represented in terms of the number and intensity of the particles, reflect the degree of MWCNT dispersion. As seen in Fig. 6, the average diameter of the acid-treated MWCNTs decreases with the acid treatment time to give 224.4, 84.8 and 55.6 nm for 12, 18, and 24 h of acid

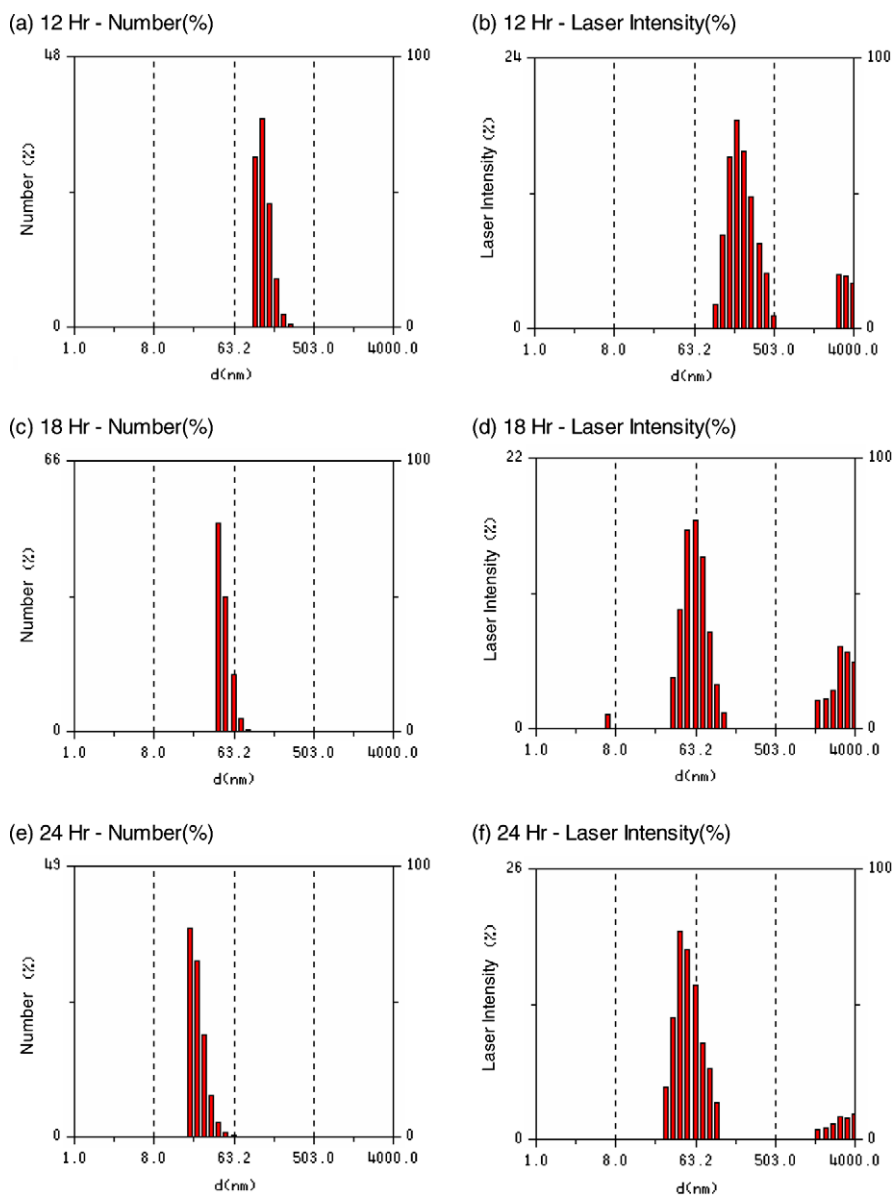


Fig. 6. DLS size distribution of carbon nanotubes dispersed in PMMA/DMF solution (MWCNTs/PMMA weight ratio at 0.025 and PMMA/DMF weight ratio at 0.0006) expressed as the number of particles and laser intensity for the acid treatment times of 12 h (a and b), 18 h (c and d) and 24 h (e and f).

treatment, respectively. It clearly demonstrates that the MWCNT dispersion is improved by the acid-treatment time.

3.4. Dispersion and percolation of carbon nanotubes in polymer matrix

Fig. 7a shows the electrical conductivity and transparency of the MWCNT/PMMA composite films cast from DMF in the glass substrate as a

function of MWCNT loading. The conductivities of the MWCNT/PMMA films cast from chloroform, toluene and THF solutions (Fig. 5) were not measurable because they were less than 10^{-16} S/cm, which was the lowest limit of our instrument. Those composite films cast from DMF containing less than 1.0 wt% of MWCNTs were non-conductive ($<ca. 10^{-16}$ S/cm). The electrical conductivity at around 2.0 wt% of MWCNT loading is 3.84×10^{-4} S/cm, which increases up to 10^{-2} S/cm

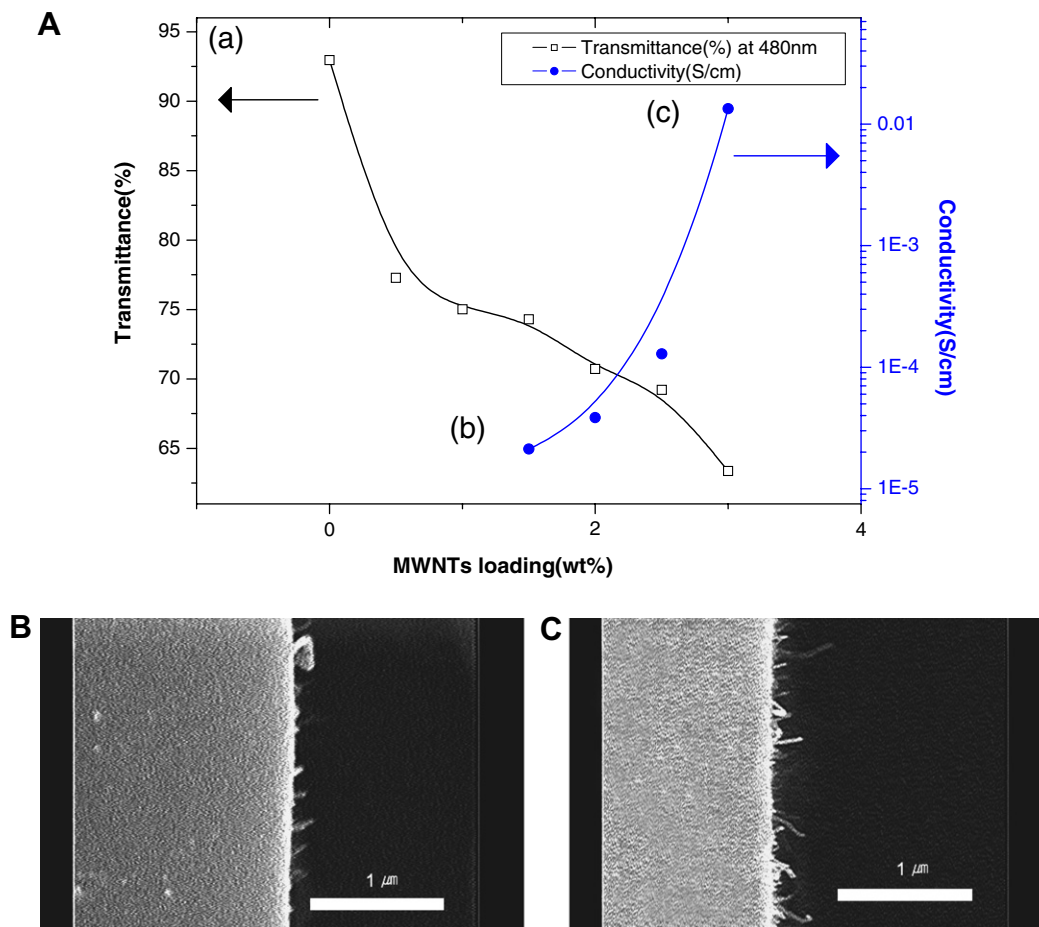


Fig. 7. Transmittance and electrical conductivity of MWCNT/PMMA composites plotted as a function of MWCNT weight fraction (a), and SEM micrographs of fractured surfaces for the 1.5 wt% (b) and 3.0 wt% composite film (c).

at 3.0 wt% of MWCNT loading, which lies among the highest in such a low loading density of MWCNTs [6,8]. We believe that the well-dispersed MWCNT/PMMA solution desirably provides a percolated state of MWCNTs at a low loading density in the PMMA matrix. Although CNT is an effective conductive filler, the electrical conductivity can be ensured by a good dispersion of CNTs in the states of both liquid mixture and solidified composite. We believe that the high conductivity achieved in our MWCNT/PMMA composite is ascribed to good dispersion of the MWCNTs carefully confirmed in both solution mixture and cast film.

The SEM micrographs of the fractured surface of MWCNT/PMMA composite films are shown in Fig. 7b and c for the MWCNT loadings of 1.5 and 3.0 wt%, respectively. As can be seen, the well-dispersed MWCNTs are pulled-out from the fractured surface and the number of pulled-out

MWCNTs increases with the increased loading density. No agglomerated MWCNT bundles were observed on the fractured surface, demonstrating that the MWCNTs should be well dispersed in the PMMA matrix.

3.5. Elimination of polymer-rich surface by mechanical polishing

As represented in the schematic in Fig. 8, even when the electrical percolation is made by the well-dispersed carbon nanotubes inside the composite film, the probing electrodes may not touch the MWCNTs at the surface due to the polymer-rich layer formed on the free surface. As schematically seen in Fig. 8a, the polymer-rich layer is usually formed at the liquid–gas interface during the solvent-casting process. When the liquid-phase PMMA/MWCNT mixture is cast as a thin film on

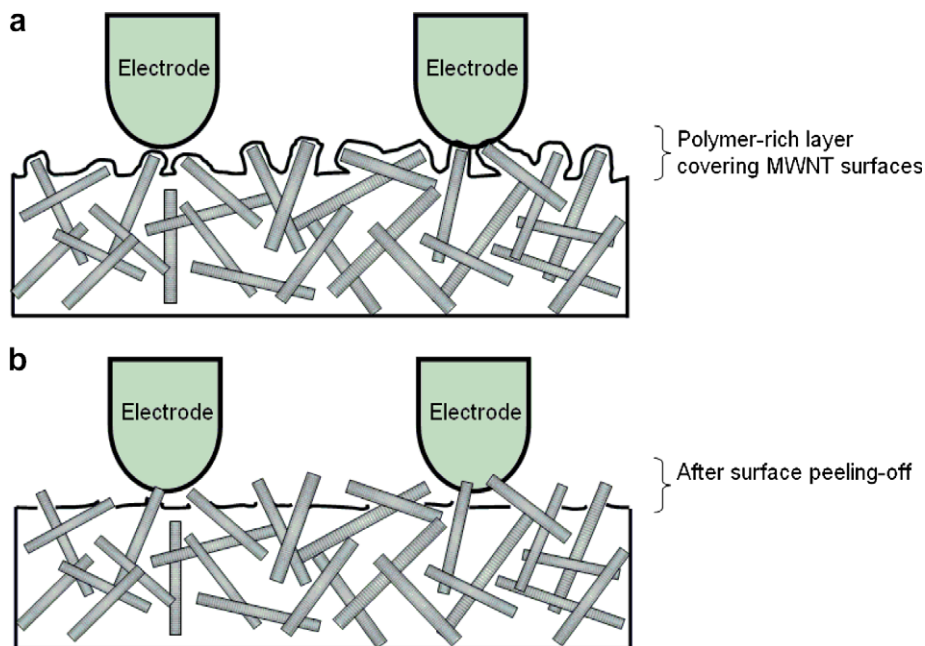


Fig. 8. Schematic of MWCNT exposure on the surface caused by mechanical polishing to eliminate the polymer-rich region on the cast film (a) before and (b) after polishing.

a substrate, the composite morphology near the surface may well be different from that in the bulk because of the surface tension and gravity force. When the polymer solution and MWCNTs have good wetting characteristics, namely having suitable

free surface energies, the MWCNTs on the free surface may well be wet (or covered) with the polymer. In addition, the density of the MWCNTs is usually higher than that of the polymer solution and, thus, the MWCNTs may sediment underneath the

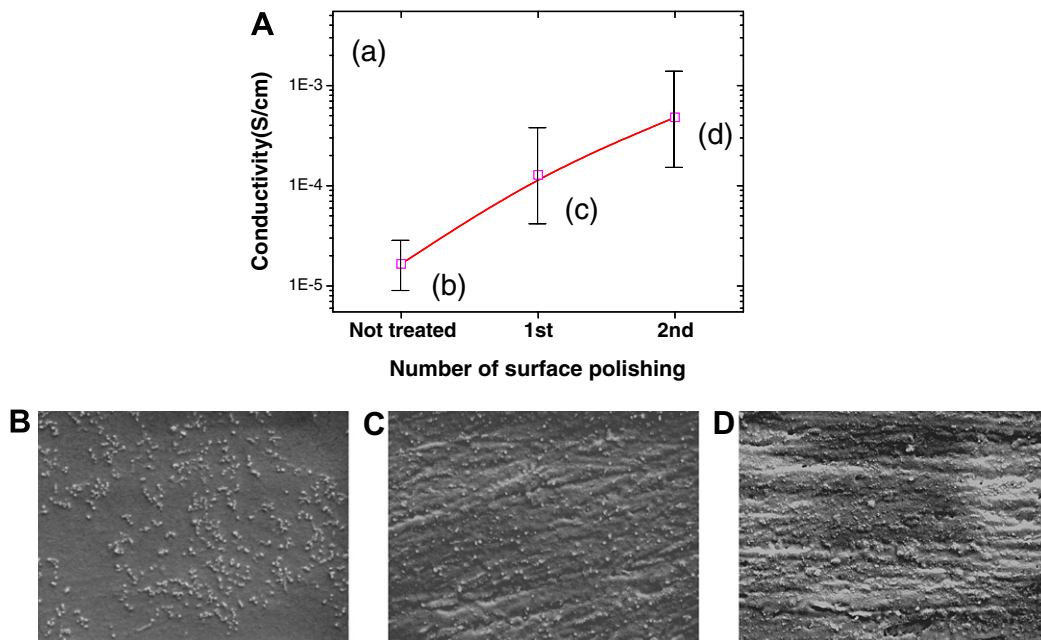


Fig. 9. Electrical conductivity of MWCNT/PMMA composites as a function of repeated mechanical polishing (a), and surface micrographs of composites film comparing (b) before polishing, (c) after 1st polishing, and (d) after 2nd polishing.

coating surface [38]. As a result, MWCNTs tend to be covered with the polymer-rich layer on the surface. Accordingly, the surface peel-off of the polymer-rich layer could improve the surface conductivity of the MWCNT composites. As schematically shown in Fig. 8b, the electrical contact between the probing electrodes and surface-exposed MWCNTs may be substantially improved simply by polishing the polymer-rich surface in a mechanical way. This consideration is supported by Fig. 9, which shows the electrical conductivity of the MWCNT composites subjected to mechanical polishing. The conductivity is elevated from about 10^{-5} S/cm to 10^{-3} S/cm with a repeated mechanical polishing for the MWCNT loading of 1.5 wt%. The SEM micrographs in Fig. 9b–d, compare the MWCNTs exposed on the surface before and after the mechanical polishing. Before the mechanical polishing, the MWCNTs appear to be covered with PMMA on the surface (Fig. 9b). With mechanical polishing, the number of MWCNTs exposed on the surface apparently increases to give more opportunity for the probing electrode to come into contact with the MWCNTs at the surface. In our experiments, the electrical conductivity was increased by approximately two orders of magnitude simply by eliminating the polymer-rich layer by mechanical polishing, without increasing the MWCNT loading.

4. Conclusion

Investigating MWCNT dispersion in different solvents and polymers, a polar aprotic solvent, DMF, showed good dispersion characteristics for the MWCNT/PMMA composites system. Increasing the acid treatment time enhanced the dispersion of the MWCNTs, because of the improved dipole interaction with the polymer and solvent. By using an adequate solution system and controlled functionalization of the carbon nanotube sidewalls, a noticeable improvement of the electrical conductivity was obtained up to 10^{-2} S/cm with 3.0 wt% of MWCNT loading. Furthermore, the polymer-rich layer on the coating surface was eliminated by mechanical polishing to give an increment of electrical conductivity approximately by the three orders of magnitude.

Acknowledgements

This work was supported by Grant No. R0120060001034802006 from the Basic Research

Program of the Korea Science & Engineering Foundation. We also appreciate the instrumental and technical support from the Samsung Advanced Institute of Technology through SAINT, Sungkyunkwan University.

References

- [1] S. Iijima, *Nature* 354 (1991) 56.
- [2] A.G. Rinzler, J.H. Hafner, P. Nikolaev, L. Lou, S.G. Kim, D. Tomanek, *Science* 269 (1995) 1550.
- [3] W.A. de Heer, A. Chatelain, D. Ugarte, *Science* 270 (1995) 1179.
- [4] P.G. Collins, A. Zettl, H. Bando, A. Thess, R.E. Smalley, *Science* 278 (1997) 100.
- [5] S. Frank, P. Poncharal, Z.L. Wang, W.A. de Heer, *Science* 280 (1998) 1744.
- [6] S.A. Curran, P.M. Ajayan, W.J. Blau, D.L. Carroll, J.N. Coleman, A.B. Dalton, *Adv. Mater.* 10 (1998) 1091.
- [7] R. Ramasubramaniam, J. Chen, H. Liu, *Appl. Phys. Lett.* 83 (2003) 2928.
- [8] F. Du, R.C. Scogna, W. Zhou, S. Brand, J.E. Fischer, K.I. Winey, *Macromolecules* 37 (2004) 9048.
- [9] T. Ogasawara, Y. Ishida, T. Ishikawa, R. Yokota, *Compos. Part. A.* 35 (2004) 67.
- [10] B. Zhu, S. Xie, Z. Xu, Y. Xu, *Compos. Sci. Technol.* 66 (2006) 548.
- [11] Y. Bin, M. Mine, A. Koganemaru, X. Jiang, M. Matsuo, *Polymer* 47 (2006) 1308.
- [12] Y.T. Sung, M.S. Han, K.H. Song, J.W. Jung, H.S. Lee, C.K. Kim, *Polymer* 47 (2006) 4434.
- [13] E. Najafi, J.Y. Kim, S.H. Han, K. Shin, *Colloid. Surf. A: Physicochem. Eng. Aspect.* 284–5 (2006) 373.
- [14] M.B. Bryning, M.F. Islam, J.M. Kikkawa, A.G. Yodh, *Adv. Mater.* 17 (2005) 1186.
- [15] F. Du, J.E. Fischer, K.I. Winey, *J. Polym. Sci.: Part B: Polym. Phys.* 41 (2003) 3333.
- [16] S. Barrau, P. Demont, E. Perez, A. Peigney, C. Laurent, C. Lacabanne, *Macromolecules* 36 (2003) 9678.
- [17] J. Rong, Z. Jing, H. Li, M. Sheng, *Macromol. Rapid Commun.* 22 (2001) 329.
- [18] M.F. Islam, E. Rojas, D.M. Bergey, A.T. Johnson, A.G. Yodh, *Nano. Lett.* 3 (2003) 269.
- [19] S.J. Park, M.S. Cho, S.T. Lim, H.J. Choi, M.S. Jhon, *Macromol. Rapid Commun.* 24 (2003) 1070.
- [20] J. Liu, M.J. Casavant, M. Cox, D.A. Walters, P. Boul, W. Lu, A.J. Rimberg, K.A. Smith, D.T. Colbert, R.E. Smalley, *Chem. Phys. Lett.* 303 (1999) 125.
- [21] K.D. Ausman, R. Piner, O. Lourie, R.S. Ruoff, M. Korobov, *J. Phys. Chem. B.* 104 (2000) 8913.
- [22] P. Poetschke, A.R. Bhattacharyya, A. Janke, H. Goering, *Compos. Interf.* 10 (2003) 389.
- [23] Y.P. Sun, K. Fu, Y. Lin, W. Huang, *Acc. Chem. Res.* 35 (2002) 1096.
- [24] C.A. Dyke, J.M. Tour, *Chem. Eur. J.* 10 (2004) 812.
- [25] V. Georgakilas, K. Kordatos, M. Prato, D.M. Guldi, M. Holzinger, A. Hirsch, *J. Am. Chem. Soc.* 124 (2002) 760.
- [26] Y. Chen, R.C. Haddon, S. Fang, A.M. Rao, P.C. Eklund, W.H. Lee, *J. Mater. Res.* 13 (1998) 2423.

- [27] J. Chen, M.A. Hamon, H. Hu, Y. Chen, A.M. Rao, P.C. Eklund, *Science* 282 (1998) 95.
- [28] M. Holzinger, O. Vostrowsky, A. Hirsch, F. Henrich, M. Kappes, R. Weiss, *Angew. Chem. Int. Ed.* 40 (2001) 4002.
- [29] J.L. Bahr, J.P. Yang, D.V. Kosynkin, M.J. Bronikowski, R.E. Smalley, J.M. Tour, *J. Am. Chem. Soc.* 123 (2001) 6536.
- [30] J.L. Bahr, J.M. Tour, *Chem. Mater.* 13 (2001) 3823.
- [31] Y. Ying, R.K. Saini, F. Liang, A.K. Sadana, W.E. Billups, *Org. Lett.* 5 (2003) 1471.
- [32] R.L. David, *Handbook of Organic Solvents*, CRC Press, Boca Raton, 1994.
- [33] L. Zhao, L. Gao, *Colloid. Surf. A: Physicochem. Eng. Aspects* 224 (2003) 127.
- [34] L. Jiang, L. Gao, J. Sun, *J. Colloid. Interf. Sci.* 260 (2003) 89.
- [35] J.Y. Lee, J.S. Kim, K.H. An, K. Lee, K.Y. Kim, D.J.D.J. Bae, *J. Nanosci. Nanotech.* 5 (2005) 1045.
- [36] M. Sano, A. Kamino, J. Okamura, S. Shinkai, *Langmuir* 17 (2001) 5125.
- [37] X. Gao, T. Hu, L. Liu, Z. Guo, *Chem. Phys. Lett.* 370 (2003) 661.
- [38] L.H. Sperling, *Introduction to Physical Polymer Science*, John Wiley & Sons, Hoboken, 2006.